J Mater Sci (2010) 45:4645–4651
DOI 10.1007/s10853-010-4676-0

ULTRAFINE GRAINED MATERIALS

Interfacial ultrafine-grained structures on aluminum alloy 6061 joint and copper alloy 110 joint fabricated by magnetic pulse welding

Yuan Zhang · Sudarsanam Suresh Babu · Glenn S. Daehn

Received: 14 February 2010 / Accepted: 28 May 2010 / Published online: 15 June 2010

Abstract Magnetic pulse welding is a solid state impact welding process, similar to explosive welding, which produces metallurgical bond by oblique high-speed impact between two metal bodies. This violent impact removes the metal surface oxide layers and then joins the two atomic level clean metal surfaces together by the incidental compression pressure. The impact velocity is at 200–400 m/s and the being welded metal surface undergoes severe plastic deformation with strain rate in the order of 10^6–10^7 s^{-1}. The ultrafine-grained structure was observed on the welded interface. This article studied two types of similar material lap joint interfaces and the base metals were aluminum alloy 6061 and copper alloy 110. Nano-indentation testing shows that the welded interfaces have significantly greater hardness than the base metals. The interface microstructure was studied by optical microscopy, electron backscatter diffraction microscopy, and transmission electron microscopy. The welded aluminum alloy 6061 interface exhibits extremely fine grains and an extremely high dislocation density. The impact welded copper alloy 110 interface presents nano-scale lamellar band structure and deformation twins. The interface hardness increasing was attributed to this impact-induced microstructural refinement.

Introduction

Traditional fusion welding results in softened heat affected zones (HAZ) because the required melting can degrade the base metal strength by dissolving strengthening precipitates or producing grain growth or recovering or recrystallizing the base metal. However, low temperature of solid state welding (SSW) techniques, especially the high strain rate impact welding processes can produce high strength and good ductility in the welded interface and surrounding region [1, 2]. In the solid state impact welding process, the materials near interface undergo severe plastic deformation (SPD) over a very short period of time. It is widely agreed that SPD processes introduce an ultrafine-grained (UFG) structure [3–7]. Therefore, UFG structures can be anticipated in impact welds. However, few studies have reported on the microstructure of an impact welded interface. This article is focused on the UFG structure fabricated by magnetic pulse welding (MPW).

MPW uses an electromagnetic pulse of very short duration (<100 μs) to accelerate a flyer plate for the high-speed oblique impact with a target plate. Besides the increased interfacial strength, the other outstanding feature of MPW is that it does not form significant HAZ. During MPW process, the flyer plate is accelerated and collides against the target plate at 200–400 m/s collision velocity [8, 9]. The surface oxide layer on the metal workpieces is believed to be removed by collision jetting [10] and the metallurgical bond is formed along the atomic level clean surfaces. Meanwhile, the impact welded interface undergoes high strain rate deformation and the estimated strain rate is about 10^6–10^7 s^{-1} [9, 11]. The MPW process can be applied for both similar material and dissimilar materials [12, 13], but this article only examined the high strain-rate-induced UFG structures on two similar material joint interfaces: aluminum alloy (AA) 6061 and copper alloy (Cu) 110.

Y. Zhang (✉) · S. S. Babu · G. S. Daehn
Department of Materials Science and Engineering,
Ohio State University, Columbus, OH 43210, USA
e-mail: zhang.561@osu.edu

Experiment

The impact welding system uses a single turn flat actuator that concentrates magnetic flux at the edge of a conductive metal flyer plate. This flyer plate sits 3.15 mm away and 12.7 mm overlap from the target plate. The actuator is coupled to a commercial 16 kJ Magneform® capacitor bank with a capacitance of 426 μF. In this study, the discharge energy of 6.4 kJ was used. Once the 6.4 kJ electrical energy is released into the MPW system, it produces a primary current pulse that approximates a damped sine wave with peak amplitude of 250 kA and rise time of 12 μs. This high-frequency alternative current passes through the actuator and induces a secondary alternative current in the adjacent metal plates. These two alternative currents have opposite phases and thus they undergo repelling force between each other. The impact velocity was measured by Photon Doppler Velocimetry (PDV) which provides submicron displacement resolution and nano-second range temporal resolution and the related strain rate was estimated based on the measured impact velocity [8, 9]. The detailed experiment setup is described in other publications [2, 14] and will not be repeated here.

Similar material welds were made from AA6061 and Cu110 and the materials chemical compositions are shown in Table 1. The age hardening AA6061 was tested in the solutionized condition produced by solutionizing at 560 °C for 20 min following by air quench. The welded plates are 0.254 mm thick, 76.2 mm wide, and 101.6 mm long. And the overlap area was ground by abrasive cloth and then cleaned by acetone. This standard surface preparation minimizes the chances of impurities degrading the welds.

Nano-indentation testing was conducted on the cross section of the welded interface. The arrows in Fig. 1a illustrated the indenter location. The indenter traversed the interface with 5 μm spacing between each other. The tested length was 50 μm on each side and the overall testing length was about 100 μm. The nano-indentation testing was carried out four times for each sample and the average hardness values were determined from separate measurements.

Table 1 Chemical composition of AA6061 and Cu110 (wt%)

Mg	Si	Cu	Fe	Cr	Mn	Zn	Ti	Al
AA6061								
0.8–1.2	0.4–0.8	0.15–0.4	<0.7	0.04–0.35	<0.15	<0.25	<0.15	Bal.
P		Cu						
Cu110								
0.015–0.04		Bal.						

Microstructure analysis was performed on electron backscatter diffraction microscopy (EBSD) and transmission electron microscopy (TEM). The samples were taken from the impact welded cross section and were metallographically polished. The final polish step was in colloidal silica suspension with the particle size of 20–60 nm. And the polished mirror-like interface was observed by EBSD. The grain boundary misorientation angle was examined by EBSD based on Kikuchi line patterns. TEM sample was prepared by focus ion beam (FIB) microscopy with final thinning voltage at 5 keV. As shown in Fig. 1b, the 200 nm thick TEM foil specimen crossed the interface and it was about 7.5 μm wide and 7.5 μm deep. This foil was then lifted out and carried by carbon film on a 3 mm diameter golden grid for TEM characterization. An FEI CM200T TEM operating at 200 kV was applied for this study.

Results and discussion

Interface hardness changes

For the joints of AA6061 and Cu110 welded at 6.4 kJ, nano-indention test quantitatively presents the joint hardness as shown in Fig. 2a–b. Comparing to the base metals, the interface region hardness values increased significantly. The strengthened region across the welded interface was quite narrow for AA6061 joint, about 20 μm wide totally. And the impact-hardened region was symmetrical with regard to the welded interface as shown in Fig. 2a. For Cu110 joint, the interface region was also strengthened compared to the base metal. Statistically the hardness profile for Cu110 was also symmetrical in Fig. 2b.

Microstructure in impact region of AA6061

The high strain rate deformation leads to interface grain refinement in MPW joint. This result is similar to various SPD processes which also lead to final equiaxed nanocrystalline structures despite the different strain paths [15]. The EBSD results from the base metals indicated that the initial grain size for AA6061 and Cu110 were 40 and 20 μm, respectively [1]. The overall TEM observations show that the grain size changes from base metal to welded interface gradually. This is shown in Fig. 3a, where the image is taken approximately 1.5 μm away from the welded interface, the grain size dropped from the approximately 40 μm base metal to sub-micrometer grain size and the diffraction patter for those grains are sharp spots as shown in Fig. 3b. Applied the same apertures setup for the region directly adjacent to the interface, the UFG structure was observed as shown in Fig. 3c. These refined

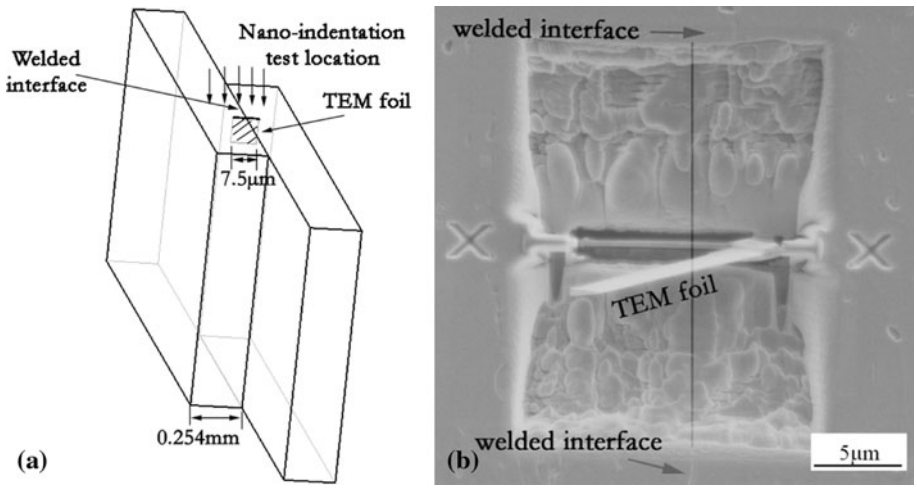

Fig. 1 **a** Illustration of the TEM specimen location and the nano-indentation testing location. The schematic is not drawn to scale. The welded plate is 0.254 mm thick and the TEM specimen is 7.5 μm wide, and 200 nm thick. **b** TEM specimen made from FIB, the *center line* indicated the welded interface location. The specimen was free stranding and tilted

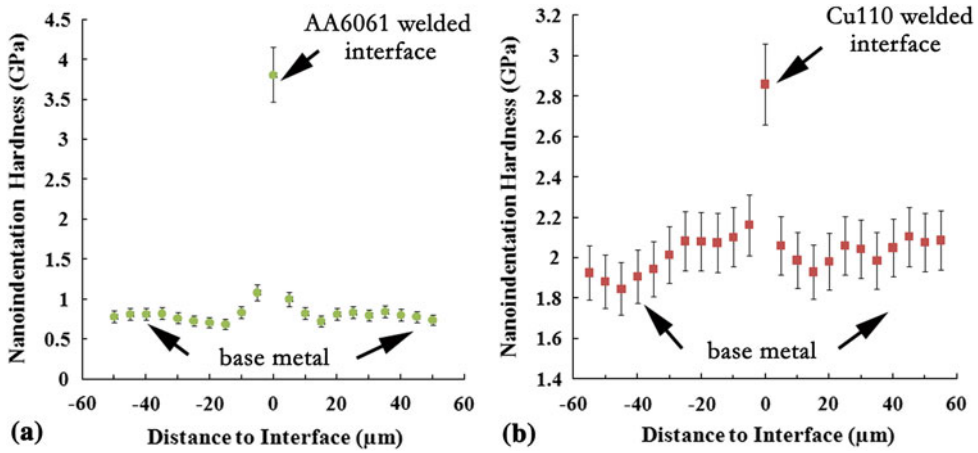

Fig. 2 Nano-indentation testing results from MPW joints. **a** AA6061 joints **b** Cu110 joints. The interface had greater hardness than the base metals

nano-crystalline structures were close to one dominant grain and the grain boundary was obvious. The refine grains were about 50 nm in diameter, while the coarse grain was in sub-micrometer. Therefore, the diffraction pattern for this region in Fig. 3d showed the Debye rings pattern from the nano-crystalline grains on top of the spots diffraction pattern from the dominant grain.

The grains size refined from micrometer to nanometer was possibly caused by rapid and severe plastic deformation. The time for the flyer plate moving from stationary state to the peak velocity was regarded as the deformation process and the PDV measured rapid deformation lasts for 10–20 μs. The plastic deformation induced heat could not dissipate quickly in this duration. The thermal and deformation profile for the interface is quite complex. There is a wavy nature of most impact welded interface and thus the local temperatures and the extents of deformation vary significantly from place to place. Pure adiabatic heating is modest. Assuming a fixed flow stress, 200 MPa, was applied for 1 mm^3 volume of the being welded AA6061 plate, and a local true strain about unity, for AA6061 (density is 2.7 g/mm^3 and specific heat capacity is 0.89 J/g °C), a temperature increase of less than 100 °C is expected. If strain levels are higher local adiabatic temperatures will rise accordingly. In many impact welds there is evidence of isolated local melting, but usually this is for a very small region of the weld interface. Since overall temperatures can be low in the transient impact welding process, little amount of recovery or recrystallization are expected. Thus the local work goes into structure refinement. Figure 3a and c also showed that the grain size changed from sub-micrometer scale to nanometer scale in a continuous manner from interface to base metal. Such grain size gradient was caused by strain and strain rate gradients which varied from the impact surface to the base metals in welding process. And the ultrafine grains were surrounded by high angle boundaries with the angles larger than 15°. These high-angle boundaries have the expected effect in increasing local hardness as shown in Fig. 2a.

The dislocations also played a key role to the grain size reduction due to subgrain formation and the high strain rate produced grain interior dislocations are observed as shown in Fig. 4a. The sub-micrometer grains in Fig. 4a were approximately 1 μm away from the welded interface and the dislocation distributed at the interior with the tendency

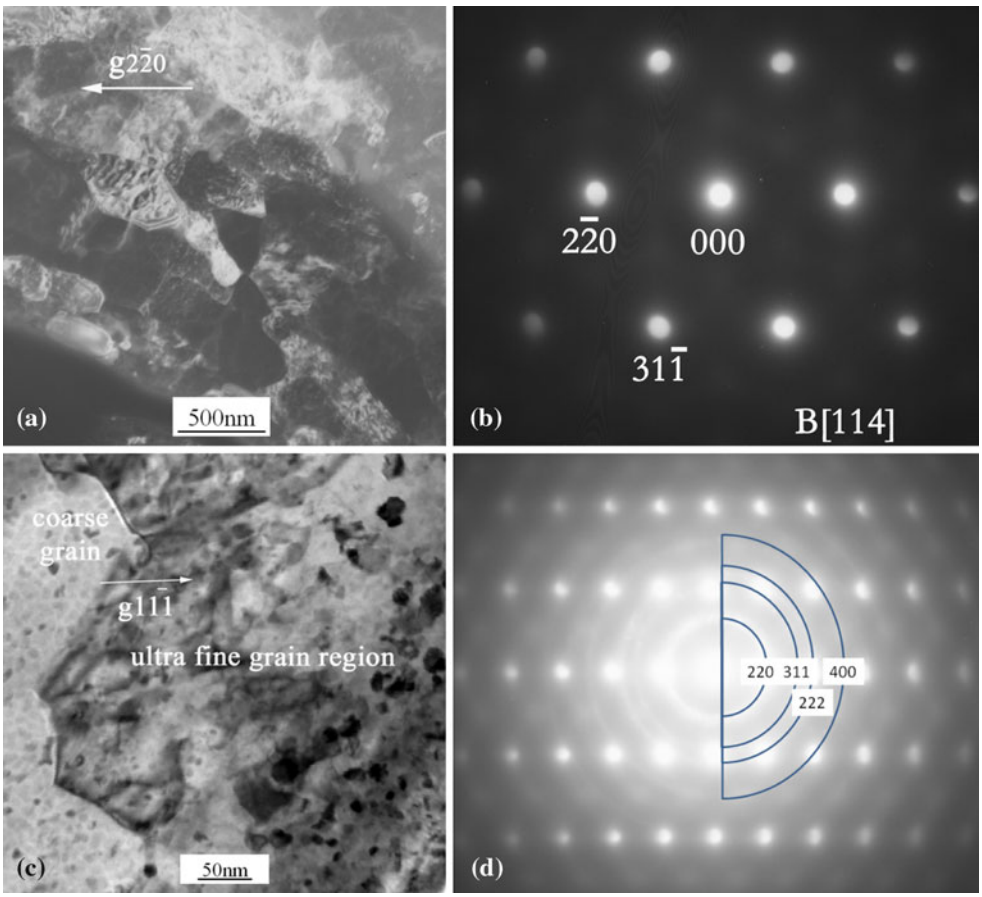

Fig. 3 TEM images and diffraction patterns from 6.4 kJ welded AA6061 joint. **a** Bright-field image on sub-micrometer grains, which were ~1.5 μm away from the interface. **b** Spot diffraction pattern from grains in (**a**). **c** Bright-field image on ultrafine grains at the welded interface. **d** Debye ring pattern on ultrafine interfacial grains

to rearrange into cellular structure as shown in Fig. 4b. This verifies that there is only dynamic recovery in the high strain-rate-induced structure. The cell walls were loosely defined but the cell interiors were almost dislocation-free. This was also reported from other SPD process [15]. TEM results at Fig. 4b also show that many parallel dislocations aligned near the grain boundaries with very small spacing. These parallel dislocations could impede consequent dislocation motion and increase the joint hardness.

Lamellar structure and deformation twins in Cu110 joint

For 6.4 kJ welded Cu110 joint, adjacent to the welded interface, lamellar bands with clearly defined boundaries dominate the structure (as shown in Fig. 5). These are in contrast to the equiaxed grain structure seen in the aluminum alloy. The direction of the lamellar band approximately followed the flyer plate impact direction. This lamellar structure has also been demonstrated in the conventional cold-rolled materials at very high strains [16, 17]. Because of the impact-loaded shock wave, there is a massive increase in local dislocation content. Figure 5 shows that the lamellar band width is less than 100 nm.

It is known that high strain rate deformation is prone to induce deformation twins in low stacking fault energy (SFE) face center cubic (FCC) structure, which would cause grain subdivision process [15, 18–21]. As a result, dislocation slip in low SFE materials was usually supplemented by twinning. For copper alloy, the SFE is low about 39 mJ/m^2, while for aluminum alloy the SFE is high about 160 mJ/m^2 [22]. Therefore, the high strain rate impact MPW process could induce deformation twins in Cu110 joints rather than in AA6061 joints. The optical images in Fig. 6b presented the evidence for the macroscopic deformation twins on the Cu110 joint. The nano-indentation testing results indicated that the joint hardness was greater than that of the as-received base metal, and it could be attributed to the occurrence of the deformation twins in the interfacial grains.

Micro twins are also clearly visible in the very fine scale as shown in the TEM image in Fig. 7a. The diffraction pattern in Fig. 7b confirms that the structure consists of

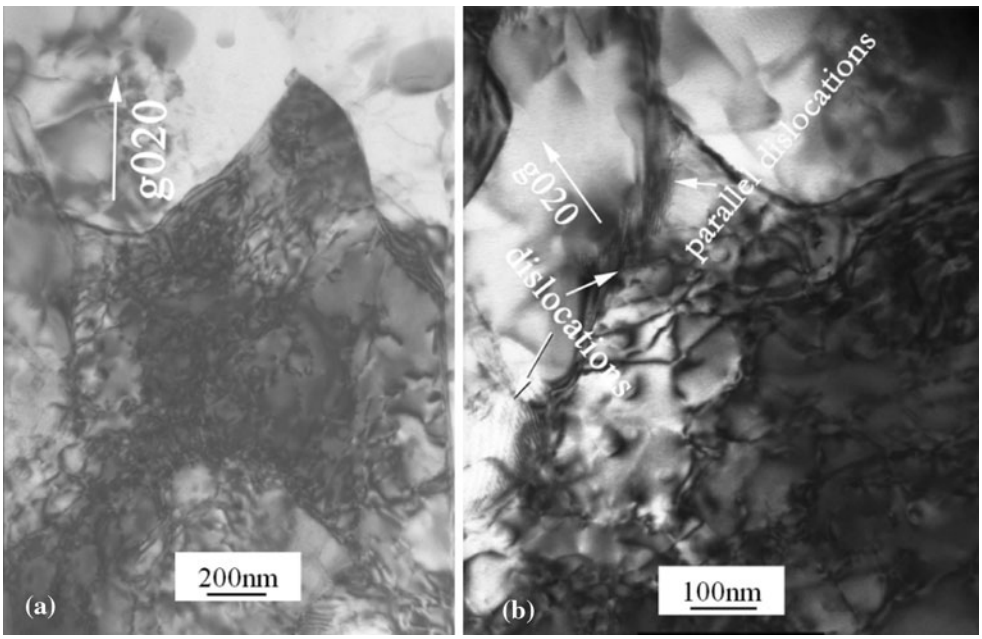

Fig. 4 Bright-field images on dislocation interaction and cellular structure in AA6061 joint. The beam direction is along [001]. **a** Dislocation interaction at the grain interior. The grains were ~1 μm away from the welded interface. **b** Cellular structure inside of the grain, the cell interior was dislocation-free. The *arrows* indicate the parallel dislocations with small spacing along the grain boundaries

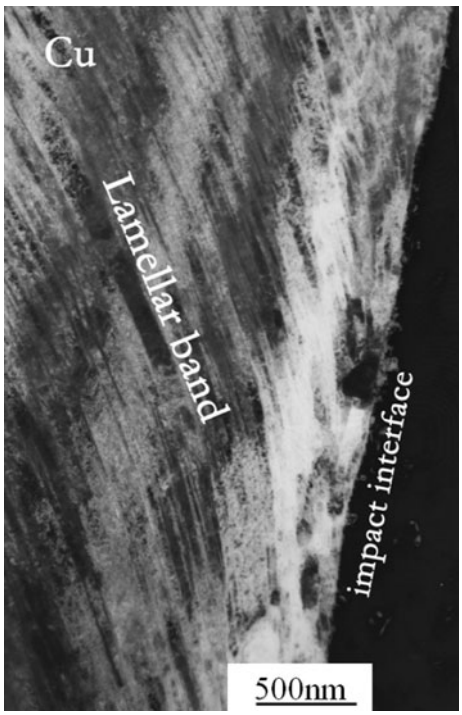

Fig. 5 Lamellar band in Cu110 joint after impact welding

deformation twins on (111) plane and along the preferential crystal orientation. The relationship between the deformation twins and the Cu110 matrix is illustrated in Fig. 7c. These nano-scale twins expanded through the narrowly spaced lamellae band structure. The width of the nano-twins observed was constant in a range about 10 nm, which is much smaller than the width of annealing twins in submicrometer [23]. During impact welding process, the shear strain rate can reach 10^6–10^7 s^{-1}, and the partial dislocations emission from the grain boundary formed mechanical twins, which suppressed the dislocation slip. Additionally, the nanometer scale lamellar band structure can be served as barriers and inhibit the dislocation slip. This result is in accord with dynamic simulations [24] that predicts such deformation twins were formed via partial dislocation emission from grain boundaries and the grain boundary junctions. All the twinning structures shown in Fig. 7 are mechanical twins, because any pre-existing annealing twins would be destroyed at this strain rate level in which the deformation twins take place [23]. These results also suggested that the deformation twins are the significant deformation mechanism for copper alloy at high strain rate impact welding process [23].

Conclusion

MPW can join metal plates together with high strain rate. The mechanical properties and microstructure evolution on the welded AA6061 and Cu110 interface were studied in this article. It was found that the welded interface hardness was greater than that of the base metals. The possible hardening mechanisms include: (1) formation of UFG

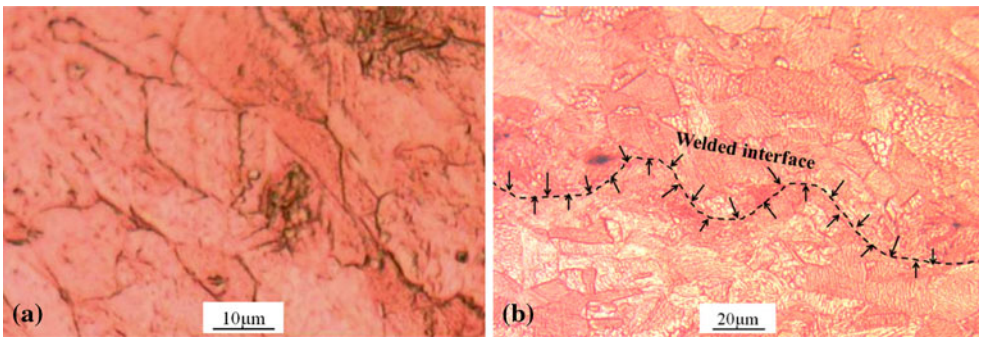

Fig. 6 Optical images from Cu110 cross section. **a** As-received Cu110. There was no twinning boundary, **b** 6.4 kJ impact welded Cu110 joint with deformation twins. The *dashed line* and the *arrows* indicate the welded interface in a wavy fashion

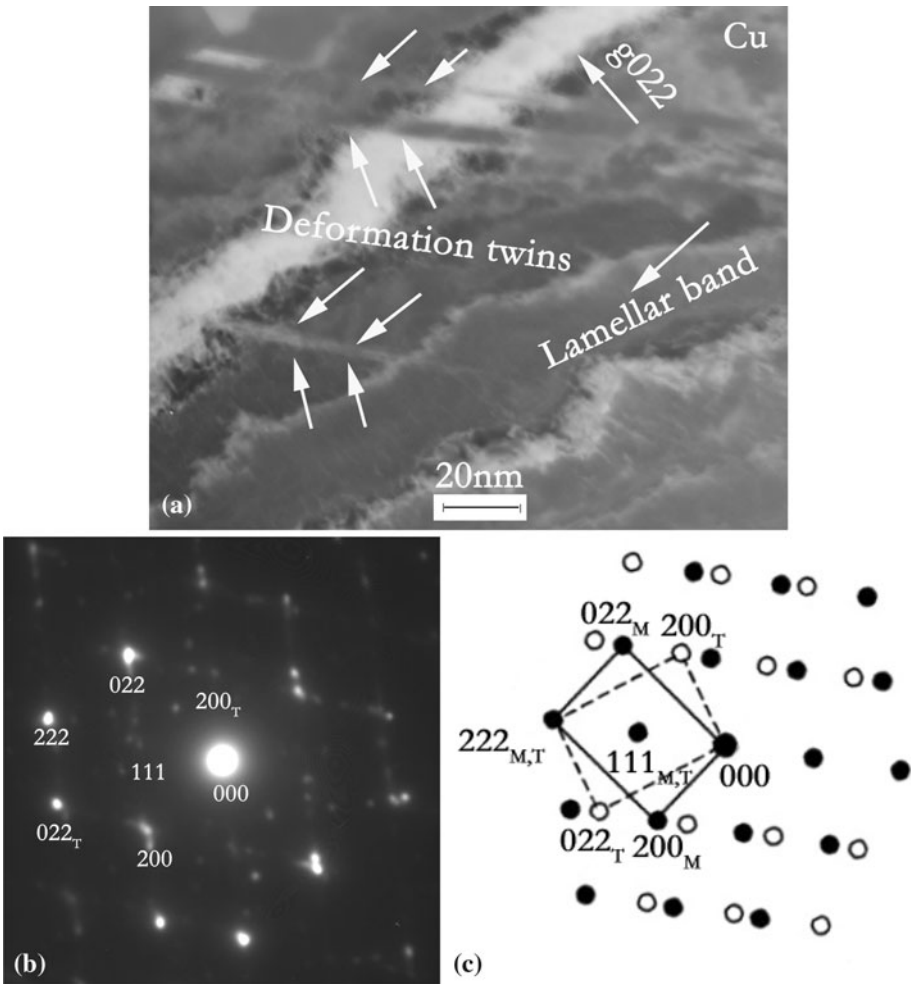

Fig. 7 Bright-field image and diffraction pattern for deformation twins in Cu110 joints. **a** Deformation twins (indicated by *arrows*) traverse the lamellar structure on Cu110 welded interface. **b** Diffraction pattern for twins obtained with electron beam on [110] direction. **c** Illustration of twinning on (111) plane

structure along the welded interface for AA6061 joint, with boundaries ranging from very high- to low-angle varieties; (2) increase of the dislocation density in AA6061 grain interior and its tendency to form cellular structure; (3) evidence of nano-scale lamellar structure and deformation twins in the impact welded Cu110 joint.

Acknowledgements The authors gratefully acknowledge the award of American welding society (AWS) graduate student fellowship for Yuan Zhang. The authors also thank to SHaRE User facility at Oak Ridge National Laboratory sponsored by the Scientific User Facilities Division, Office of Basic Energy Sciences, U.S. Department of Energy. We also thank Sang Hoon Shim for his great help on nano-indentation testing at Oak Ridge National Lab.

References

1. Zhang Y et al (2008) Sci Technol Weld Join 13(5):467
2. Zhang Y et al (2010) J Mater Process Technol. doi:10.1016/j.jmatprotec.2010.01.001
3. Iwahashi Y et al (1998) Acta Mater 46(9):3317
4. Hayes JS, Keyte R, Prangnell PB (2000) Mater Sci Technol 16:1259–1263
5. Tsuji N et al (2002) Scripta Mater 46(4):305
6. Valiev RZ et al (2002) J Mater Res 17(1):6
7. Morris DG, Gutierrez-Urrutia I, Muñoz-Morris MA (2007) J Mater Sci 42(5):1439. doi:10.1007/s10853-006-0564-z
8. Zhang Y et al (2008) In: 10th international LS-DYNA users conference simulation technology, 2008, Dearborn, MI
9. Johnson JR et al (2009) Metal Form 80(5):359
10. Masumoto I, Tamaki K, Kojima M (1985) Trans Jpn Weld Soc 16(2):110
11. Lee KJ et al (2007) Mater Sc Eng A 471(1–2):95
12. Hokari H et al (1998) Weld Int 12(8):619
13. Aizawa T, Kashani M, Okagawa K (2007) Weld J 86:119s
14. Zhang Y, Babu SS, Daehn GS (2010) In: 4th international conference on high speed forming, 2010, Columbus, OH. Handle-ID: http://hdl.handle.net/2003/27194
15. Zhilyaev AP et al (2008) J Mater Sci 43(23):7451. doi:10.1007/s10853-008-2714-y
16. Hughes DA, Hansen N (2001) Phys Rev Lett 87(13):135503
17. Hughes DA et al (1995) Wear 181:458
18. Bussiba A et al (2001) Mater Sci Eng A 302(1):56
19. Mishra RS et al (1999) Scripta Mater 42(2):163
20. Komura S et al (1998) Scripta Mater 38(12):1851
21. Andrade U et al (1994) Acta Metall Mater 42:3183
22. Ogata S, Li J, Yip S (2002) Science 298(5594):807
23. Huang X (2007) J Mater Sci 42(5):1577. doi:10.1007/s10853-006-0988-5
24. Yamakov V et al (2002) Nat Mater 1(1):45